AADE-17-NTCE-041

Prediction and Identification of Downhole Drilling Vibrations Through an Advanced Drillstring Model

Mohsen Emami, Qian Li, Ian Soukup, Sheila McLean, National Oilwell Varco

Abstract

Downhole vibration during drilling operations is considered as one of the main impediments of the drilling process and is a major concern to drillers. The most severe instances of axial, torsional, and lateral vibration can lead to bit bounce, stick slip, and whirl, respectively, which create large cyclic stresses leading to fatigue. Consequently, these vibrations can shorten the service life of the drillstring, downhole and surface equipment, and can cause catastrophic failures. Vibrations also consume energy transferred into the drilling process, and as such, decrease drilling efficiency.

This paper develops an efficient finite element method (FEM) based model that effectively captures the essential vibrational behavior of the drillstring during any drilling process. The model's theoretical capability in predicting lateral, axial, and torsional natural frequencies is compared with data from two laboratory test rigs and several high-frequency drilling datasets captured at differing depths from three wells. The FEM-based model can predict all types of drillstring vibrations. On average, comparisons between the model and real data correlate within 4% for natural frequencies that include several modes and harmonic ranges. Additionally, the model has a thorough set of critical drilling parameters that can be calibrated for any drilling scenario for better predictions.

The model has been deployed in several laboratory and field applications and has been successfully used to identify the circumstances when harmful vibrations are initiated. This new model and similar mathematical tools provide innovative opportunities through advanced model-based control to improve drilling efficiencies and decrease drilling times throughout the entire well construction process.

Introduction

Vibrations can consume a large portion of the energy transmitted into the drilling system (i.e., decrease drilling efficiency). They can also increase bit-wear rate, and in extreme circumstances, cause catastrophic effects on the drillstring and drilling equipment. As such, drillstring and drill bit vibrations that occur while drilling are of primary concern to the driller [1]. Drillstring vibration modes can be axial, torsional, and lateral, which can lead to bit bounce, stick slip, and whirl, respectively. Furthermore, each of these vibration modes can lead to varying destructive effects on drilling equipment, causing disparate drilling inefficiencies [2]. The vibrational destructive nature can also lead to poor borehole quality, resulting in a magnitude of negative consequences, such as stuck drilling pipe, lost circulation, hole deviation, pipe failures, and borehole instability [3]. Identifying vibration and differentiating among the vibration modes while drilling is critical so that corrective measures can be taken before their negative repercussions occur.

In many cases, surface measurements alone are insufficient to identify the dynamics of the entire drillstring. Severe axial and lateral vibrations near the bit may show no visible vibrations at surface [2]. Using wired drillpipe to instrument the drillstring and capture data while drilling can circumvent these issues partly. Sensors integrated along the drillstring can capture added detail about its dynamic behavior; however, wellbore interactions and vibration nodes can still mask damaging vibrations located in uninstrumented regions of the drillstring. Best results are achieved from a combination of physics based models and empirical data sets. Model based prediction that consumes downhole tool data from wired pipe for feedback is ideal and highly preferred when possible for both real-time control and pre/post analytics.

With advanced modeling, the response of the entire drillstring can be calculated to predict the vibrational behavior of the system. The model predictions can then be used to drive decision making either directly through driller-dependent functions or autonomously by model-based control. Modeling can be used in concert with a sensor suite to validate data quality and predict surface measurements to downhole responses. Several equipment providers have already deployed predictive mathematical models to forecast and mitigate drilling vibrations. One software application provides automated vibration dampening to reduce torsional vibration and stick-slip oscillations while drilling [4]. Another company's model is used to predict natural frequencies of the drillstring and bottom hole assembly (BHA) [2]. The model described herein has over 20 output parameters (often called synthetic measurements) that define physical states of the drillstring, wellbore, and drilling fluids. Many of these parameters can be used as comparators or correctors to measurements made while drilling from surface, downhole or along string measurements.

Modern drillstring models focus on different mathematical techniques that are generally classified as follows: lumped parameter models, neutral-type time-delay models, and distributed parameter models. Lumped parameter models

idealize the drillstring as a mass-spring-damper system, consist of one or more degrees of freedom (DoF), and consider coupled torsional-axial-lateral dynamics [5]. Lumped parameter models are defined by ordinary differential equations (ODEs) in a conceptually simplified manner, streamlining their implementation of control systems. Though lumped parameter models are conceptually and computationally straightforward, they do not address nonlinear wellbore contact and geometric nonlinearities in coupled vibration [6]. Also, a discretized approach using a lumped model that incorporates numerous lumped mass elements to represent the drillstring can complicate the solution to the coupled ODEs and result in prolonged and complicated model solutions. This method of deploying a lumped parameter drillstring model is generally not as efficient or as accurate as the distributed parameter approach using FEM techniques [7].

Neutral-type time-delay models are derived from distributed parameter models, but use time-delay theory to simplify the equations and reduce the boundary value problem to a neutral-type time-delay equation. Equivalent input-output models, derived from the wave equations, are a suitable method to manage relatively simpler models involving only the primary interest variables [5].

Models using the distributed parameter approach utilize FEM to solve a system of differential equations that characterize drilling variables in an infinite-dimensional setting. A series of simpler elements and their defining ODEs are combined through FEM to define the system's global behavior. While model complexity is a tradeoff for model accuracy, fewer elements can result in efficient and timely solutions [5].

This paper develops an FEM-based model that effectively captures the fundamental vibrational behavior of the drilling process. Comparisons are made of natural frequencies found in laboratory tests and actual drilling data with model-estimated frequencies. The FEM model can predict all the types of vibration, and thus can be used to prevent the circumstances that initiate harmful vibration. The model, once integrated with drilling equipment and control systems, can mitigate equipment damage, improve borehole quality, and increase drilling rate of penetration (ROP). It has been proven that, with mathematical models, better wells can be drilled faster by maximizing the efficient energy transfer from the surface rig machines downhole to the position where the drill bit is contacting the rock [8]. The next section provides an overview of the FEM-based model, followed by an in-depth discussion of a frequency analysis performed on this model and actual drilling data.

Mathematical Model

In this study, FEM is the key paradigm to perform frequency analysis. Basically, FEM breaks a complicated continuous system into several simpler elements. Then, it is straightforward to develop ODEs of motion with known boundary conditions and applied forces. Equations of motion for these elements can be written in matrix-form ODEs called local matrices. FEM combines those equations of motions together and creates a global matrix form ODE that describes a system's dynamical behavior. In this approach, increasing the number of elements decreases the errors introduced in the model. However, it also increases the computational complexity of the algorithm through increasing the size of the global matrix.

In the proposed model, beam elements with 12 DoF are used. This type of element provides an efficient and accurate method to predict detailed dynamical behavior of tubulars. The equations of motion of the $\boldsymbol{i^{th}}$ element can be written as:

$$[M_i]\{\ddot{e}_i\} + \dot{\Omega}[G_i]\{\dot{e}_i\} + [K_i]\{e_i\} = \{Q_i\} \quad (1)$$

where M_i, G_i, and K_i are 12×12 local mass, gyroscopic, and stiffness matrices of the i^{th} element and $\{e_i\}$ is the deformation vector. An element stiffness matrix is composed of four parts given by [9]:

$$[K_i] = [k_i^e] + [k_i^a] + \left[k_i^{\varphi}\right] + [k_i^{as}] \quad (2)$$

where k_i^e, k_i^a, k_i^{φ}, and k_i^{as} are elastic, axial, torsional, and axial stiffening matrices, respectively [9]. Similarly, an element mass matrix consists of four parts, namely translational, rotary, torsional, and coupled torsional-transverse inertia mass matrices, given by [9]:

$$[M_i] = [m_i^t] + [m_i^r] + \left[m_i^{\varphi}\right] + [m_i^e] \quad (3)$$

Detailed descriptions of the element local matrices and derivation methods have been documented [9-11]. All local equations matrices can be assembled together and the drillstring model can be expressed as follows [1]:

$$[M]\{\ddot{e}\} + \dot{\Omega}[G]\{\dot{e}\} + [K]\{e\} = \{Q\} \quad (4)$$

where M, G, and K are global mass, gyroscopic, and stiffness matrices, respectively. Also, e and Q are $6(N_e + 1)$ vectors containing, respectively, position and force information of all the element nodes where N_e is the total number of elements used in model. Frequency analysis is performed based on Eq. (4).

Natural Frequency Prediction Using FEM-Based Model

Mechanical systems tend to oscillate at their natural frequencies in the absence of external forces. Theoretically, there are infinite natural frequencies for any continuous mechanical system. However, a certain number of those natural frequencies occur in the working frequency range. The importance of natural frequencies is that when a system is excited at a frequency equal to one of its natural frequencies, the amplitude of oscillation tends to increase infinitely if there is no damping in the system. Since, in reality, all mechanical systems have some degree of damping in their atomic level, and also in contact with surrounding fluids/objects, the oscillation amplitude would never go to infinity. However, the amplitude of oscillations can be high enough to breakdown the mechanical system after a certain number of oscillations. Therefore, having the ability to predict natural frequencies of the drillstring is crucial, so they can be avoided during any drilling procedure.

FEM-based models can predict natural frequencies of continuous mechanical systems. This section discusses the

natural frequencies calculated by the FEM-based model and compares them with laboratory data and drilling measurement results to test the theory and the implementation of the model.

Prediction of natural frequencies for similar systems published in literature.

Though the FEM model developed for full-scale drillstrings, predicting natural frequencies of downscaled systems can effectively test FEM theory and its implementation. Several laboratory tests on downscaled drilling rigs have provided experimental data for natural frequencies of the tested systems [10, 12-13]. The main advantage of downscaled drilling rigs is that they can be rotated by a wide range of surface rotation speeds, often measured in revolutions per minute (RPM), of which their system behavior can be analyzed precisely. Also, the geometry of the test can be controlled more accurately as the string shape can be inspected visually to match the desired path. Whereas, in an actual drilling scenario, the drillstring path cannot be controlled precisely and the surface rotation speed takes a narrower range.

Figures 1 and 2 demonstrate two laboratory drillstrings used to validate their physical information along with the simulator model.

String: Solid steel rod
Length: 1.44 m
Outer diameter: 6 mm
Rotation speed: 50-1,000 RPM
Motor coupling: Elastic coupling with a swivel-base universal joint
Fluid types: Air, water, turpentine oil
Boundary condition: Clamped-Clamped

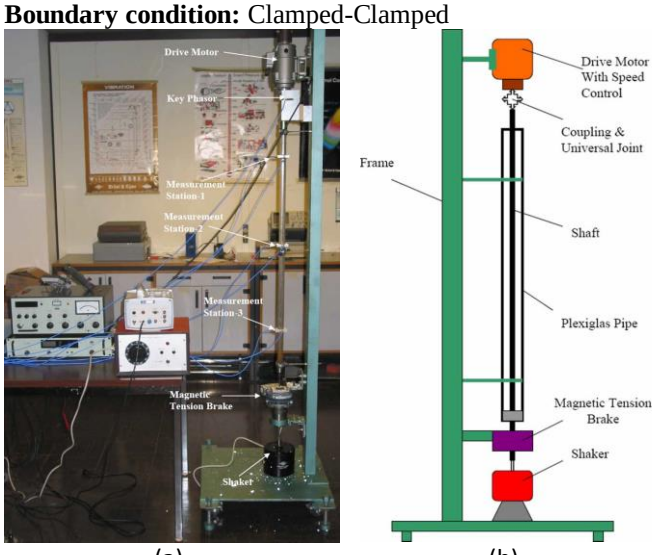

Figure 1: Khulief and Al-Sulaiman laboratory drillstring (a) and its schematic (b) [10].

String: Solid steel rod
Length: 1.485 m
Outer diameter: 3 mm
Maximum rotation speed: 1,000 RPM
Motor coupling: Elastic coupling with a swivel-base universal joint
Fluid types: Air, water
Boundary condition: Clamped-Clamped with two bearings at $z = 0.072$ m and $z = 1.37$ m

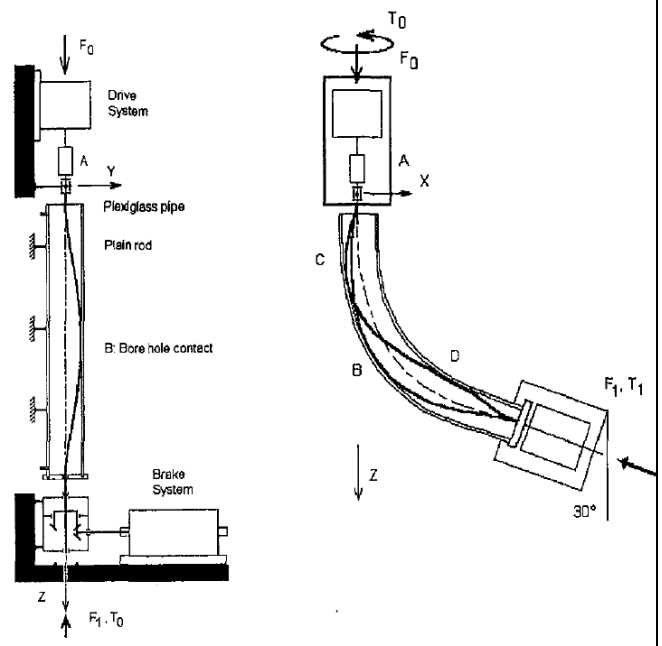

Figure 2: Berlioz et al. laboratory drillstring [12].

Physical parameters of these downscaled rigs were fed to the drillstring in the FEM-based model and boundary conditions of the model were adjusted to match the reported restrictions in the papers. Natural frequency analysis results are shown in Tables 1 and 2 along with the previously measured results [10]. Khulief and Al-Sulaiman [10] reported three lateral natural frequencies of their downscaled rig measured in air, water, and turpentine oil. Since the effect of different fluids is applied separately in our FEM formulation, only the results measured in air are used for comparison (because air has marginal dampening effects on the drillstring due to its minimal viscosity).

Table 1: Lateral natural frequencies compared to results in [10].

Rot. Sp. (rad/s)	Experimental results measured in: air	water	turpentine oil	FEM results	Error compared to air results
ω_1	41.72	37.87	38.63	42.28	1.34%
ω_2	156.86	151.22	152.69	153.84	-1.96%
ω_3	345.95	336.73	338.96	338.75	-2.08%
			Average absolute error:		1.79%

Table 2: Lateral natural frequencies compared to results in [12].

Rot. Sp. (rad/s)	Experimental results measured in air	FEM results	Error
ω_1	43.35	45.26	4.41%
ω_2	120.61	124.75	3.43%
ω_3	234.32	245.12	4.61%
		Average error:	4.15%

As shown in Tables 1 and 2, natural frequencies predicted by the simulator are close to those gathered from experimental studies. Average errors of the estimated values are 1.79% and 4.15%, compared to [10] and [12], respectively.

Figure 3 demonstrates the first three mode shapes of the two downscaled drilling rigs, which shows the physical model used in the FEM-based model can provide a close estimation of drillstring dynamics.

Another advantage of the natural frequency test is that it can reveal the minimum number of elements required for the FEM-based model to provide acceptable results. Table 3 shows the natural frequencies of the model for a system in [10] with a different number of elements. From this study, it can be seen that after ten elements, the calculated natural frequencies are insensitive to the number of elements. Therefore, for this case, ten elements are enough to predict the dynamic and vibration of the system accurately.

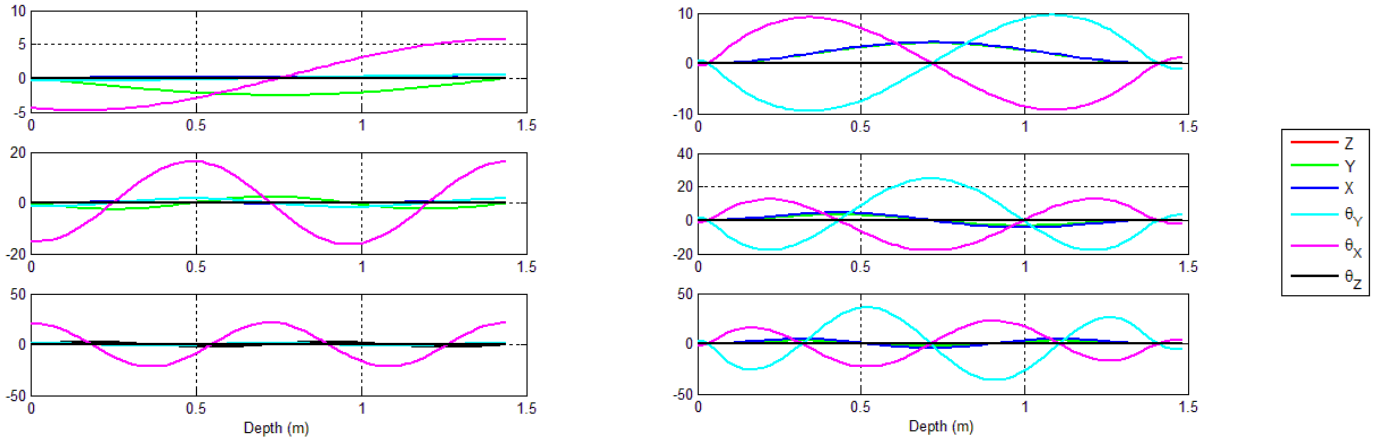

(a) (b)

Figure 3: First three lateral natural frequency mode shapes calculated for (a) [10] and (b) [12].

Table 3: Model natural frequencies with different number of elements for system in [10]

Element number	1	2	5	10	20	35	50	80	100	150
ω_1 (rad/s)	45.8	42.4	42.3	42.3	42.3	42.3	42.3	42.3	42.3	42.2
ω_2 (rad/s)	173.8	168.8	154.0	153.8	153.8	153.8	153.8	153.8	153.8	153.8
ω_3 (rad/s)	469.8	404.8	341.0	338.9	338.7	338.7	338.7	338.7	338.7	338.7

Drilling rig data frequency analysis and comparison to FEM-model results

Analyzing high-speed rig data of greater than 50 Hz in the frequency domain can help quantify the signal's energy patterns distributed across frequencies and extract information, which includes rig data noise, natural frequencies of the drillstring, and properties of applied forces. The usefulness of the analysis depends on cleanliness of data and its sampling rate. High levels of noise and low vibration magnitudes can make it difficult or even impossible to extract meaningful information out of data. Model validation through natural frequency comparison is essential to demonstrate model accuracy. Predicting natural frequencies and resonances of the system is critical to understanding and controlling the excitation/dynamic response of the drillstring. Therefore, a model that has a good correlation between the calculated natural frequencies and measured natural frequencies can accurately predict drillstring behavior.

Vibration analysis in this section consisted of studying the frequency response of the system for axial and torsional resonances. This was accomplished by analyzing each dataset within the frequency domain and capturing the frequencies that produced associated peaks in magnitude from the signal response. Specific dataset measurements were used to differentiate between the axial resonances and the torsional resonances.

For frequency analysis on drilling data, 10–20 minute segments of drilling data at 20 different depths over three wells were studied. The 20 depths included data during both rotating

(18 datasets) and sliding (two datasets) drilling modes. The data segments were spaced so that drilling content was captured in different trajectories (vertical, curve, lateral) of the well and with different rotational speeds. There were two or three instruments that continuously measured data during the construction of these wells, a surface sensor and one or two downhole subs. The surface sensor was positioned at the top of the drillstring and integrated into the upper internal blowout preventer. The lower downhole sensor was positioned 30−40 ft from the bit and the second sensor was positioned about 5,000 ft from the bit. This arrangement ensured a more complete analysis of downhole dynamics and provided the measured response along the drillstring assembly.

It was deemed beneficial to analyze data with near constant RPM and ROP; therefore, sections of data with minimal fluctuations of these parameters were selected. The data from the downhole instruments was sampled at 50 Hz and stored in memory, while the data from the surface sensor was sampled at 128 Hz and stored on a local server. Typically, analysis of frequencies of less than one-eighth of sampling frequency is considered reliable in the industry. For this application, sampling rates provided by these sensors (50 Hz or 128 Hz) were useful for analysis of frequencies below 6.25 Hz (375 RPM). Intensive data processing and time synchronization were required to accurately extract meaningful data from months of hole construction.

The instruments measured four dynamics responses quantified in engineering terms as axial load, axial acceleration, torsional load, and rotational velocity. Each dataset included between 8 and 12 high-frequency data channels for torsional- and axial-related data. The surface sensor measured the axial load through a strain bridge that sensed the axial and circumferential strain of a column-style spring element. The downhole sensors measured the axial strain of a mechanical diaphragm and utilized the output of a half strain bridge.

Torsional loads were measured by the shear strain bridges in both tools. Rotational velocities were measured using a MEMS gyroscope in all three instruments, which provided both positive and negative magnitudes. It was evident from the analysis that the rotational outputs provided the cleanest frequency response data. This was due to lower rotational capacities of the equipment leading to higher sensing resolution and signal-to-noise ratio. For example, the rotational sensors have capacities of +/-250 RPM and display general frequency response magnitudes of greater than 0.5 RPM for the first few resonances. The axial vibration is the most difficult to identify because it has the smallest signal-to-noise ratio. The axial capacities of the sensors are 1000 kip and 300 kip for the surface and downhole sensors, respectively. The frequency response magnitudes can be less than 500 lb, resulting in a signal-to-noise ratio of more than double that of the rotational measurement.

Surface and downhole axial loads were used to determine the axial resonances. Surface and downhole torque, as well as surface and downhole rotational velocities, were used to determine the torsional resonances. The data was processed in a manner that minimized bias errors by discretizing the signal into smaller sections of data and normalizing the data.

Figure 4 shows the profiles of three South Texas wells selected in this study. Its table lists measured depths (MD) of the three wells from which drilling datasets were taken. Note that the majority of the data was collected while in the rotating drilling mode, with the exception of two cases in which the data was taken while sliding, as designated with an (S).

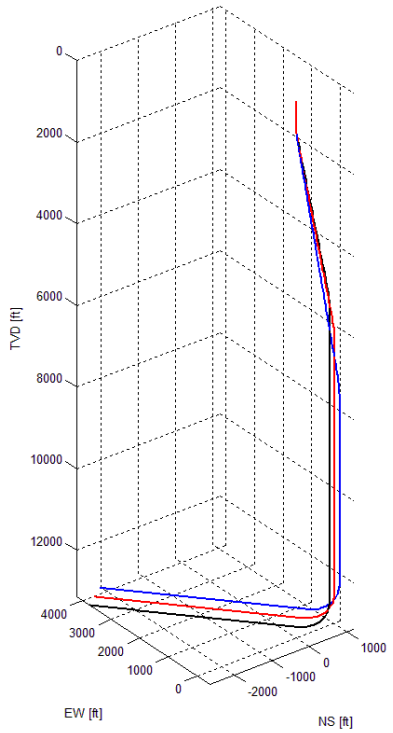

Drilling Data Depth [ft]		
Well 1 (blue)	**Well 2 (red)**	**Well 3 (black)**
7,052.5	5,410.4 (S)	4,189.8
8,640.1	9,850.3	8,339.1
10,444.0	10,527.0 (S)	10,233.8
12,593.0	10,653.3	12,116.1
14,203.0	12,723.7	14,283.9
17,261.0	13,264.3	14,593.8
---	14,648.8	14,872.7

Figure 4: Profiles of three South Texas wells studied in this paper and drilling data depths.

Drilling data at different selected times was visually analyzed to ensure consistency of the results. Figure 5 demonstrates frequency analysis on two channels with low-quality (a) and high-quality (b) data.

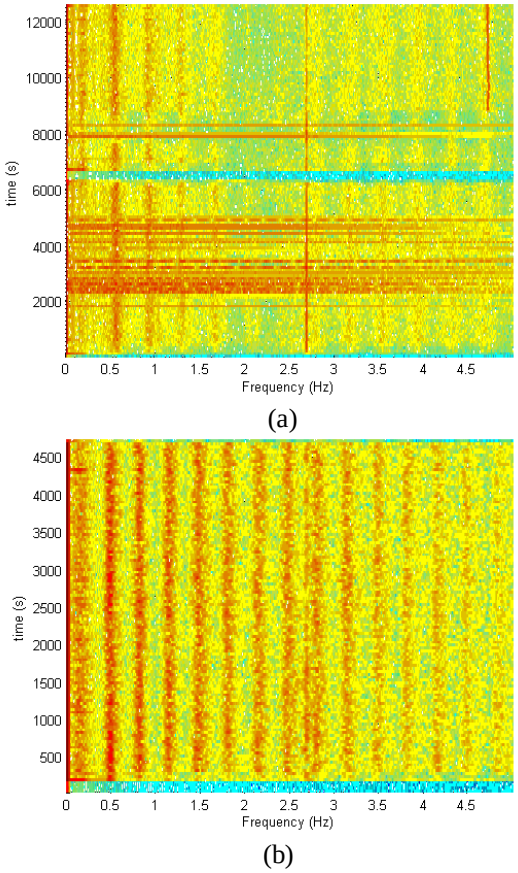

Figure 5: Torsional frequency analysis on channels with low-quality (a) and high-quality (b) data.

In Figure 5, the amplitude of each frequency is shown by color; red with maximum and dark blue with minimum energy. Note that the total length of the drillstring between top drive and bottom of the hole determines the dynamic behavior of the drillstring—not the hole depth. Theory suggests that when the bit is on bottom, natural frequencies are almost constant for different weights on bit (WOBs) and surface RPMs (in the drilling range). Since length of the drillstring is constant over each dataset, natural frequencies of the drillstring are expected to be changing with an extremely slow rate during drilling operations. As such, the expectation is to detect (almost) vertical red regions at natural frequencies throughout the entire drilling time, similar to what is seen in Figure 5(b). Also, dominant excitation frequencies are anticipated to be consistent over short time periods. As shown in Figure 5(a), in few cases sections of high-frequency data have low quality and dominant frequencies cannot be observed. Therefore, drilling data frequency analysis results should be visually examined before plotting in two dimensions for the purpose of selecting the dominant frequencies. There are usually more than one high quality torsional data channel at each time. Our tests showed, dominant frequencies in different channels of torsional data are consistent with less than 2% difference.

Most rotational data gathered from rotating drilling was clean enough to extract meaningful frequency information. However, few axial channels were found with enough observability for analysis. Also, both datasets extracted from the sliding modes were found unusable; basically, the variation of the signal compared to noise was not large enough. Consequently, frequency analysis did not extract the dominant signal frequency in these cases. This is because in the sliding mode, the drillstring and BHA are stationary in most directions, and are only sliding along the axis of the well. Since sensors are placed above the BHA, bit oscillations are dampened by friction and fluid forces before reaching the sensors.

Figure 6 illustrates a torsional frequency analysis of a sliding dataset compared to a rotating one. Different colors show drillstring torque at differing depths. As demonstrated in Figure 6(a), the frequency analysis in the sliding mode shows a high level of noise-to-signal ratio compared to Figure 6(b), the analysis performed on drilling data in the rotating mode. Frequency analysis performed on data from the sliding sections indicate that the signals were not of high enough amplitude to measure above the extraneous excitation perturbations. Therefore, frequency analysis of the sliding datasets was discarded.

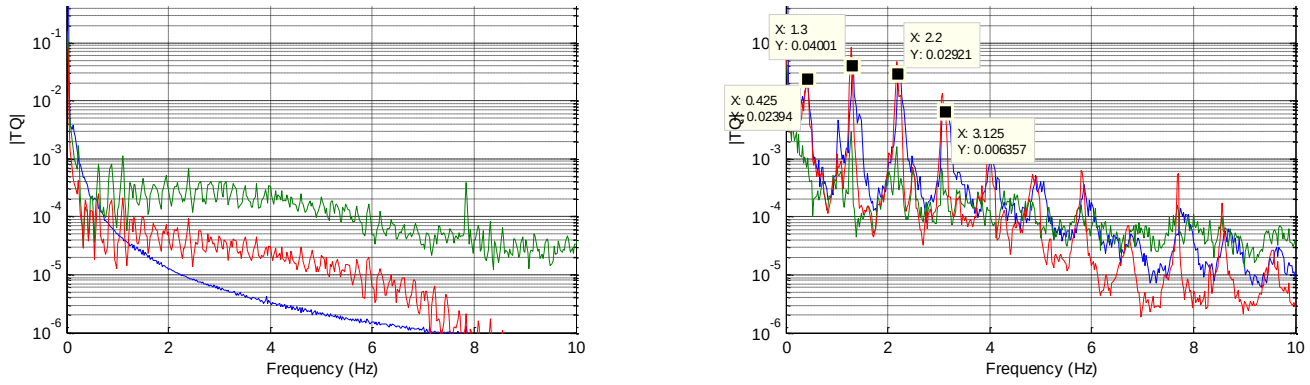

Figure 6: Torsional frequency analysis of sliding drilling (a) and rotating drilling (b). Blue, red, and green colors show torque measurements at different sensor subs located at surface, mid-string, and the BHA. respectively.

Datasets provided in this paper represent different depths and borehole types, with the latter including both vertical and lateral drilling sections. Table 4 shows torsional and axial natural frequency analyses on one of the drilling datasets (i.e., Well 2 captured at 10,653.3 ft.). Similar to this dataset, frequency analysis results showed that the torsional resonances were most easily captured because they dominated the frequency spectrum, while the axial resonances were in many cases dominated or disturbed by the excitation frequency that occurred at a frequency of once per revolution of drillpipe. In the worst cases, all axial natural frequency had to be discarded due to the disturbances from the axial excitation forces. As demonstrated in Table 4, the natural frequencies estimated by the FEM-based model are close to those found from the frequency analysis of the actual drilling data.

Table 4. Frequency analysis on Well 2 at depth 10653.3 ft.

	Torsional study			Axial study		
	Dominant frequencies in drilling data (Hz)	FEM natural frequencies (Hz)	Difference in percentage	Dominant frequencies in drilling data (Hz)	FEM natural frequencies (Hz)	Difference in percentage
ω_1	----	0.210	----	----	0.339	----
ω_2	0.6307	0.631	0.07%	1.005	1.017	1.19%
ω_3	1.073	1.054	-1.78%	----	1.697	
ω_4	1.5	1.479	-1.37%	2.384	2.379	-0.21%
ω_5	1.943	1.908	-1.82%	3.295	3.064	-7.01%
ω_6	2.39	2.339	-2.15%	3.895	3.752	-3.67%
ω_7	2.808	2.772	-1.29%	----	4.443	----
ω_8	3.277	3.207	-2.13%	----	----	----
ω_9	3.725	3.644	-2.17%	----	----	----
ω_{10}	4.201	4.082	-2.82%	----	----	----
	Average absolute (difference):		1.73%	Average absolute (difference):		3.02%

Figure 7 illustrates the torsional frequency analysis results on the three wells and the corresponding errors. On average, the FEM-based model underestimated the torsional natural frequencies by 1.42% on all three wells.

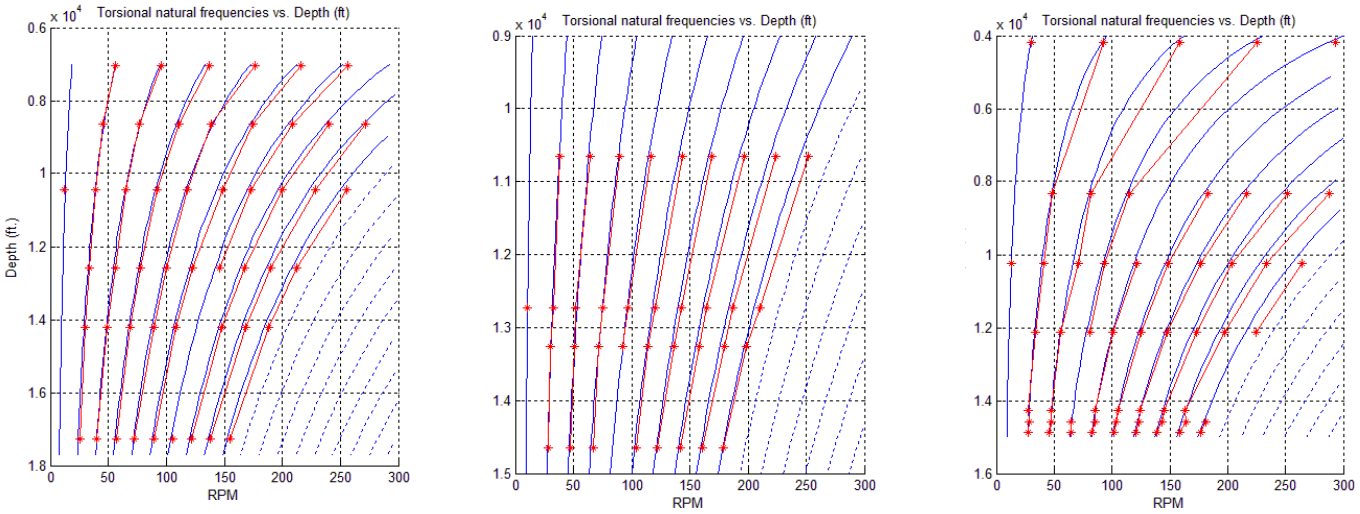

(a) Well 1, average error: 1.85%, STD: 8.5×10-3

(b) Well 2, average error: 1.55%, STD: 9.4×10^{-3}

(c) Well 3, average error: 1.63%, STD: 1.2×10^{-2}

Figure 7: Torsional frequency analysis results on Well 1 (a), Well 2 (b), and Well 3 (c).

Excitation frequencies and sensor resolution masked the lower harmonics in the axial modes. As a result, only a few depths from Wells 2 and 3 could be selected with confidence. Table 5 lists the axial natural frequency analysis results for six datasets. It demonstrates that the axial natural frequency prediction with the FEM-based model has, on average, a 4.16% difference with the drilling data. The authors think part of this difference can be attributed to error in data frequency analysis due to the inadequate sensitivity of the sensors that measured the dynamic axial loads. On average, a 3.9% difference exists between the axial natural frequency predictions with dominant frequencies found in drilling data.

As demonstrated in Table 5 and Figure 7, model accuracy in predicting natural drillstring frequencies is consistent along different depths. This indicates that the model can predict vibration behavior of the drillstring in curved and horizontal sections as well as the vertical section. This shows that the FEM-based model closely predicts the natural frequencies of the system, and therefore, can calculate the dynamic behavior of the drillstring in different borehole geometries and through the entire well construction process.

Table 5. Axial frequency analysis on Wells 2 and 3.

	Well 2 Results				**Well 3 results**							
	MD: 10,653.3		**MD: 14,648.8**		**MD: 10,233.7**		**MD: 12,116.1**		**MD: 14,283.9**		**MD: 14,593.8**	
	Exp.	**Model**	**Exp.**	**Model**	**Exp.**	**Model**	**Exp.**	**Model**	**Exp.**	**Model**	**Exp.**	**Model**
ω_1	---	0.339	---	0.248	---	0.353	---	0.297	---	0.254	---	0.249
ω_2	1.005	1.017	0.843	0.744	1.112	1.059	---	0.891	---	0.764	0.732	0.748
ω_3	---	1.697	---	1.241	---	1.766	1.35	1.488	1.25	1.274	---	1.247
ω_4	2.384	2.379	---	1.739	2.476	2.477	---	2.087	---	1.785	1.651	1.747
ω_5	3.295	3.064	---	2.238	---	3.190	2.68	2.689	---	2.297	---	2.248
ω_6	3.895	3.752	2.913	2.738	---	3.906	---	3.294	---	2.810	---	2.751
ω_7	---	4.443	---	3.240	---	4.625	3.86	3.902	3.54	3.326	3.12	3.255
ω_8	---	---	3.757	3.744	---	---	---	4.513	---	3.842	---	3.760
Avg. Difference		**3.02%**		**6.03%**		**2.41%**		**3.89%**		**3.97%**		**4.08%**

CONCLUSIONS

In this study, an FEM-based model for drillstring simulations during well construction is presented. The physical equations governing the structure of the model are defined and the model performance including its ability to capture drillstring vibrations is described. Natural frequencies and associated harmonics calculated by the model were qualified against two independent test cases: 1) the natural frequencies observed in downscaled laboratory drilling rigs and 2) dominant frequencies observed in drillstring while drilling 18,000-ft horizontal wells. It was shown that the model calculations correlate within 4% of measured natural frequencies across several modes and harmonic ranges. These results validate the mathematical theory as well as the implementation of the numerical techniques used to idealize the drillstring response during well construction. Successful applications of similar mathematical tools used to mitigate damaging vibrations and improve drilling efficiency were reviewed, indicating that this model will provide new opportunities to advance drilling methods. The FEM-based model, once integrated with drilling equipment and control systems or simply used for advisory systems and well planning purposes, can mitigate drilling equipment damage, improve wellbore quality, and increase drilling rates, providing for an improvement in drilling efficiencies and overall well economics.

Acknowledgments

The authors would like to thank National Oilwell Varco for permission to publish this paper.

References

1. S. M. Bashmal, Finite element analysis of stick-slip vibrations in drillstring. King Fahd University Of Petroleum & Minerals, Dhahran, Saudi Arabia, Master of Science Thesis, April 2005.
2. [2] Schlumberger, Drillstring Vibrations and Vibration Modeling. https://www.slb.com/~/media/Files/drilling/brochures/drilling_opt/drillstring_vib_br.pdf, 2010.
3. J. J. Azar, PEH: Drilling Problems and Solutions. PetroWiki, http://petrowiki.org/PEH%3ADrilling_Problems_and_Solutions, December 2014.
4. National Oilwell Varco, SoftSpeed II Stick-Slip Prevention Service. http://www.nov.com/softspeedii/, 2015.
5. M. B. S. Marquez, I. Boussaada, H. Mounier, and S. I. Niculescu, Analysis and Control of Oilwell Drilling Vibrations: A Time-Delay Systems. Springer, 2015.

6. M. T. Piovan and R. Sampia, Non Linear Model for Coupled Vibrations of Drill-Strings. Mecánica Computacional, 25, 1751-1765, 2006.
7. P. M. Thompson, Technical Report: e-WildCat AutoDriller Analysis. unpublished, August 2013.
8. F. Efteland, A. Coit, and K. Mckenna, Surface Control Software Dramatically Mitigates Downhole Torsional Vibration in the Eagle Ford Shale Play as Validated by High-Speed Downhole Dynamics Data. Society of Petroleum Engineers, January 2014.
9. H. A. Alnaser, Finite element dynamic analysis of drillstring. King Fahd University of Petroleum & Minerals, Dhahran, Saudi Arabia, Master of Science, 2002.
10. Y. A. Khulief and F. A. Al-Sulaiman, Laboratory investigation of drillstring vibrations. Journal of Mechanical Engineering Science, 2249-2262, 2009.
11. Q. Jing, Modeling and simulation for design of suspended MEMS. PhD dissertation, Carnegie Mellon University, Pittsburgh, Pennsylvania, USA, 2003.
12. A. Berlioz, J. Der Hogopian , R. Dufour, and E. Draoui, Dynamic behavior of a drillstring: experimental investigation of lateral instabilities. Journal of Vibration and Acoustics, 118 (3), 292–298, 1996.
13. T. V. Aarrestad and A. Kyllingstad, An experimental and theoretical study of coupled boundary conditions for vibrations in drillstrings. Society of Petroleum Engineers, Richardson, Texas, USA, January 1986.